PHYSICAL REVIEW B VOLUME 42, NUMBER 15 15 NOVEMBER 1990-II

Electronic structure of disordered alloys: Korringa-Kohn-Rostoker cluster coherent-potential approximation

S. S. A. Razee, S. S. Rajput, R. Prasad, and A. Mookerjee*
Department of Physics, Indian Institute of Technology, Kanpur 208016, India

(Received 21 February 1989; revised manuscript received 3 July 1990)

A self-consistent cluster theory, the Korringa-Kohn-Rostoker cluster coherent-potential approximation (KKR-CCPA), is presented to study the electronic structure of the random, substitutionally disordered metallic alloys. This theory combines the augmented-space formalism and conventional Korringa-Kohn-Rostoker methods to determine the effective medium self-consistently. One advantage of this method is that it preserves Herglotz properties of the configuration-averaged Green's function needed to calculate various electronic properties, such as charge densities, essential for full charge self-consistency. Unlike the single-site approximations, the KKR-CCPA introduces diagonal as well as off-diagonal corrections in the scattering matrices. The formulation has been applied to a model one-dimensional alloy. We find that the density of states in the KKR-CCPA is somewhat structured, due to correlated scattering from clusters of atoms.

I. INTRODUCTION

Most of the current studies on electronic properties of random substitutionally disordered metallic alloys are done within single-site approximations, in which the real disordered system is replaced by a translationally symmetric effective medium with an effective scatterer on each site. The effective scatterer is then determined by averaging over all the possible configurations of a single real atom embedded in the effective medium. The two most commonly used single-site approximations are the average-t-matrix approximation and the coherent-potential approximation (CPA).[1-3] In the average-t-matrix approximation, the effective scattering matrix is the average of those of the alloy constituents. In the CPA, the effective medium is determined by a self-consistency condition, which requires that the average scattering from a single real atom embedded in the effective medium be zero. It is generally agreed that the CPA is the best single-site approximation. However, it might fail whenever a single-site effective-medium description becomes inadequate, e.g., in the presence of strong local environmental effects, such as short-range order and clustering tendencies. These local environmental effects can be investigated, accurately and convincingly, only through a cluster or multisite approximation. Recent experimental works on CuPd (Refs. 4 and 5) and CuPt (Refs. 5 and 6) systems show that the CPA is not adequate for these systems.

With the realization of the need to go beyond the CPA, several attempts have been reported.[7-24] These attempts can be broadly classified into two categories: non-self-consistent cluster approaches[11-14] and self-consistent cluster approaches.[7-10,16-24] In the non-self-consistent approach, there has been a considerable amount of work within the tight-binding framework. But, to our knowledge, only the work of Gonis *et al.*[12,13] is within the conventional Korringa-Kohn-Rostoker (KKR) framework. In this work, a cluster consisting of a central site and its shell of nearest neighbors was embedded in an effective medium determined within the KKR-CPA method. The density of states (DOS) was then obtained from the site-diagonal element of the Green's function at the center of the cluster. The effective medium, however, was not determined self-consistently with respect to the cluster. It was expected that the effects of the cluster self-consistency would be small. However, the work of Stefanou *et al.*[25] on CuPd systems shows that these effects may be significant.

In the self-consistent cluster approach also, a great deal of work has been done, mostly on the tight-binding models,[7-10,16-18] though a few papers have appeared on muffin-tin models[22-24] also. Some of these approaches are either too difficult to implement computationally, such as the molecular CPA,[8] or they lack proper physical behavior.[7,9,15] Traveling cluster approximation[17] and augmented-space formalism[26,27] (ASF) are the only approaches which have been proved to be analytic, while preserving the conservation laws and sum rules.[18,28,29] The ASF, originally developed in the tight-binding framework, provides a self-consistent cluster coherent-potential approximation (CCPA) in which one can go beyond the CPA in a systematic way.[16] In this method, the effective medium is determined by the self-consistency condition that the average scattering from all the possible configurations of a real cluster embedded in the effective medium be zero. Unlike the molecular CPA, the CCPA gives a translationally invariant effective medium.[29] There is a vast literature on the ASF (Refs. 18-21 and 26-28) and it has been used extensively for electronic structure calculations in the tight-binding framework.[21]

The ideas of ASF are rather general and can be incorporated within the conventional KKR method as well.[24] Although a formula for averaged DOS using Lloyd's formula[3,30] has already been developed,[24] it does not allow the calculation of charge densities and, therefore, the prospect of doing charge self-consistency is ruled out. Furthermore, it is now generally agreed that the electronic properties of an alloy should be calculated by the Green's-function method, as the formulas based on Lloyd's formula may give unphysical results,[30,31] such as negative DOS and negative spectral density. Our formulation is based on the Green's function and therefore overcomes these difficulties: using it one can calculate charge density and therefore can achieve charge self-consistency within the local-density approximation of the density-functional theory.

This theory can also treat a random ternary alloy. Work within the tight-binding framework has already been reported.[32] An extension of the theory to deal with nonrandom effects like short-range order has also been reported in the tight-binding framework.[33] We have extended it using the KKR framework and our calculations are in progress. Therefore we plan to discuss the nonrandom effects in a separate paper.

The outline of the paper is as follows. We present our formulation in Sec. II. In Sec. II A we briefly discuss the main ideas of the ASF. In Sec. II B we combine the ASF and the conventional KKR method to formulate the KKR-CCPA formalism. It is found that the KKR-CCPA introduces diagonal as well as off-diagonal corrections in the scattering matrices of the effective medium. In Appendix A we present simplification of the KKR-CCPA equations for clusters of one atom and two atoms. We also show that, for a one-atom cluster, the KKR-CCPA equations reduce to the familiar KKR-CPA equation, which is the correct limit. In Sec. II C we give the expressions for the configuration-averaged Green's function and various quantities which can be obtained from it, such as DOS and charge densities. The problem of impurities embedded in the effective medium has also been discussed in this section. As a first attempt to implement KKR-CCPA, we have applied it to a one-dimensional model alloy as presented in Appendix B. This model is chosen because it has analytical expressions for various quantities[34] and thus is computationally simpler. In Sec. III we present the results of our calculations of DOS within KKR-CPA and KKR-CCPA. We also present local DOS on impurities for a cluster of two real impurities embedded in the KKR-CPA medium. We compare the KKR-CCPA DOS with these local DOS's on the impurities and show that their features are correlated. This suggests that the structures in the KKR-CCPA DOS are due to correlated scattering from the clusters of atoms. We also present the averaged DOS on the central site of a cluster of atoms embedded in the KKR-CPA medium, for clusters of two, three, and five atoms. These calculations are similar to the embedded cluster calculations of Gonis *et al.*[13] We find that this averaged DOS reproduces some of the structures of the KKR-CCPA DOS, which become prominent as we increase the cluster size.

II. FORMULATION

A. The augmented-space formalism

The ASF (Refs. 26 and 27) is an efficient and convenient method for configuration averaging a quantity, which is a function of a set of random variables $\{n_i\}$, provided the probability distribution $p(\{n_i\})$ is known explicitly. The configuration average of a function $\underline{A}(\{n_i\})$ is the integral

$$\langle \underline{A} \rangle = \int \underline{A}(\{n_i\}) p(\{n_i\}) \prod_i dn_i \; . \tag{2.1}$$

For a random substitutional alloy with no short-range order, the composite probability distribution $p(\{n_i\})$ can be written as a product of the individual single-site probability distributions $p_i(n_i)$, i.e.,

$$p(\{n_i\}) = \prod_i p_i(n_i) \; . \tag{2.2}$$

If we assume that $p_i(n_i)$ has finite moments to all orders, then it is always possible to write $p_i(n_i)$ as the matrix element[26]

$$p_i(n_i) = -\frac{1}{\pi} \mathrm{Im} \langle f_0^{(i)} | (n_i \underline{I} - \underline{M}^{(i)})^{-1} | f_0^{(i)} \rangle \; , \tag{2.3}$$

where $\underline{M}^{(i)}$ is an operator in the configuration space ϕ_i of rank m, spanned by $\{|f_j^{(i)}\rangle\}$, $j=0,1,2,\ldots,m-1$, with m being the number of components of the alloy. The configuration space ϕ_i contains all the possible configurations for the site i and $|f_0^{(i)}\rangle$ is referred to as the ground state in ϕ_i. The basis $\{|f_j^{(i)}\rangle\}$ can be defined if $p_i(n_i)$ is known explicitly. For a random binary alloy $A_x B_y$, $p_i(n_i)$ can be written as

$$p_i(n_i) = x\delta(n_i - 1) + y\delta(n_i) \; ,$$

where

$$n_i = \begin{cases} 1 & \text{for } i = A \\ 0 & \text{for } i = B \; . \end{cases} \tag{2.4}$$

It immediately follows from Eq. (2.4) that $p_i(n_i)$ satisfies the required conditions, namely,

$$\int p_i(n_i) n_i^l dn_i \text{ finite for } l = 0,1,2,\ldots$$

and

$$p_i(n_i) \geq 0 \; . \tag{2.5}$$

For $p_i(n_i)$ as defined in Eq. (2.4), $\underline{M}^{(i)}$ is a tridiagonal matrix in the space ϕ_i of rank 2 spanned by $|f_0^{(i)}\rangle$ and $|f_1^{(i)}\rangle$ with a representation[26]

$$\underline{M}^{(i)} = \begin{bmatrix} x & \sqrt{xy} \\ \sqrt{xy} & y \end{bmatrix} . \tag{2.6}$$

It is easily seen that

$$\underline{M}^{(i)} | f_0^{(i)} \rangle = x | f_0^{(i)} \rangle + \sqrt{xy}\, | f_1^{(i)} \rangle \; ,$$

and

$$\underline{M}^{(i)} | f_1^{(i)} \rangle = y | f_1^{(i)} \rangle + \sqrt{xy}\, | f_0^{(i)} \rangle \; .$$

The bases $|f_0^{(i)}\rangle$ and $|f_1^{(i)}\rangle$, referred to as the ground state and the excited state in the configuration space, respectively, are given by

$$| f_0^{(i)} \rangle = \sqrt{x}\, |\mathcal{A}\rangle_i + \sqrt{y}\, |\mathcal{B}\rangle_i$$

and

$$|f_1^{(i)}\rangle=\sqrt{y}\,|\mathcal{A}\rangle_i-\sqrt{x}\,|\mathcal{B}\rangle_i\ . \tag{2.7}$$

The bases $|\mathcal{A}\rangle_i$ and $|\mathcal{B}\rangle_i$ indicate the occupancy of the ith site. By the augmented-space theorem[26] we get

$$\langle\underline{A}\rangle=\langle F|\underline{\tilde{A}}(\{\underline{M}^{(i)}\})|F\rangle\ , \tag{2.8}$$

where $|F\rangle=\prod_i|f_0^{(i)}\rangle$ and represents a state in the configuration space $\Phi=\prod_i\phi_i$. The remaining bases in the configuration space are those for which there are excited states $|f_1^{(i)}\rangle$ on one or more sites. These are conventionally written as $|F_s\rangle$, where s is a composite index of one or more sites on which we have $|f_1^{(i)}\rangle$, while on the rest of the sites we have $|f_0^{(i)}\rangle$. For example, a state $|F_{jk\ldots l}\rangle$ is given by

$$|F_{jk\ldots l}\rangle=\prod_i|f_n^{(i)}\rangle\text{with } n=\begin{cases}0 & \text{for } i\neq j,k,\ldots,l\\ 1 & \text{for } i=j,k,\ldots,l\ .\end{cases} \tag{2.9}$$

$\underline{\tilde{A}}(\{\underline{M}^{(i)}\})$ is an operator in the augmented space $\psi=\mathcal{H}\otimes\Phi$, where $\mathcal{H}$ is the Hilbert space spanned by $\{|i\rangle\}$. The augmented space is spanned by $\{|i,F_s\rangle\}$ and its rank is $N\times2^N$, where N is the total number of atoms in the solid. The operator function $\underline{\tilde{A}}(\{\underline{M}^{(i)}\})$ is the same function of $\{\underline{M}^{(i)}\}$ as $\underline{A}(\{n_i\})$ is of $\{n_i\}$.[26] Note that Eq. (2.8) is exact, but cannot be used for computational purposes. Therefore we look for some approximation which will reduce the rank of the augmented space. The simplest approximation is the CCPA, in which a small cluster $\mathcal{C}$ is chosen out of $\{i\}$ and the complement of the cluster is taken as an effective medium. The randomness comes only within $\mathcal{C}$ and so the configuration averaging is done over all the possible configurations of the cluster. We get the self-consistent CCPA equations from the condition that the configuration-averaged Green's function obtained by this technique is equal to the Green's function of the effective medium. Depending upon the size of the cluster we can generate various kinds of effective medium. For example, if we take a one-atom cluster we will get the CPA condition. Thus our formulation offers a convenient and systematic way of going beyond the CPA.

B. The KKR-CCPA

In this section we discuss the application of the augmented-space technique to the KKR Green's-function[1,2,30] method of calculating electronic structure for a system of muffin-tin potentials. The Hamiltonian for such a system can be written (in atomic units) as

$$H=-\nabla^2+\sum_i v_i(\mathbf{r}-\mathbf{R}_i)\ , \tag{2.10}$$

where v_i are the muffin-tin potentials centered at the position of the sites, $\mathbf{R}_i$. The Green's function for this system is given by[30]

$$\begin{aligned}\underline{G}(\mathbf{r},\mathbf{r}';E)=&\sum_{LL'}\underline{Z}^{\,i}_{L}(\mathbf{r}_i)\underline{T}^{\,ij}_{LL'}\underline{Z}^{\,j}_{L'}(\mathbf{r}'_j)\\ &-\delta_{ij}\sum_{L}\underline{Z}^{\,i}_{L}(\mathbf{r}_i)\underline{J}^{\,i}_{L}(\mathbf{r}'_j)\ ,\end{aligned} \tag{2.11}$$

where $\mathbf{r}$ and $\mathbf{r}'$ lie on ith and jth cells, respectively. The wave functions $\underline{Z}^{\,i}_{L}(\mathbf{r}_i)$ and $\underline{J}^{\,i}_{L}(\mathbf{r}_i)$ are, respectively, the regular and irregular solutions of the differential equation,[30]

$$[-\nabla^2+v_i(\mathbf{r}_i)-E]\underline{Z}^{\,i}_{L}(\mathbf{r}_i)=0\ , \tag{2.12}$$

and $\underline{T}^{\,ij}_{LL'}$ are on-the-shell matrix elements of path operators given by

$$\underline{T}^{\,ij}_{LL'}=(\underline{A}^{\,-1})^{ij}_{LL'}\ ,$$

where

$$\underline{A}^{\,ij}_{LL'}=\underline{C}^{\,i}_{LL'}\ \delta_{ij}-\underline{B}^{\,ij}_{LL'}\ , \tag{2.13}$$

and $\underline{C}^{\,i}_{LL'}$ is the inverse of the on-the-shell single scatterer t matrix. Suppressing the angular momentum indices we can write

$$\underline{T}^{\,ij}=[(\underline{C}^{\,i}\underline{I}-\underline{B})^{-1}]^{ij}\ , \tag{2.14}$$

where $\underline{B}$ is the matrix with elements $\underline{B}^{\,ij}$ which depend only on the lattice structure[3] and do not contain any randomness, while $\underline{C}^{\,i}$ carry the information about randomness. The nonrandomness of the off-diagonal terms $\underline{B}^{\,ij}$, in the KKR framework, in contrast to the tight-binding framework, where randomness comes both in the diagonal as well as off-diagonal terms, makes the application of the ASF to the KKR framework theoretically much simpler. The first step towards implementing the ASF to the present problem is to write $\underline{C}^{\,i}$ in terms of the random variable n_i, i.e.,

$$\underline{C}^{\,i}=\underline{C}^{\,B}+\delta\underline{C}n_i\ ,$$

where

$$\delta\underline{C}=\underline{C}^{\,A}-\underline{C}^{\,B}\ . \tag{2.15}$$

From Eq. (2.13), the matrix $\underline{A}$ can be written as

$$\begin{aligned}\underline{A}&=\sum_i\underline{C}^{\,i}|i\rangle\langle i|-\sum_{i,j(i\neq j)}\underline{B}^{\,ij}|i\rangle\langle j|\\ &=\underline{C}^{\,B}\sum_i|i\rangle\langle i|+\delta\underline{C}\sum_i|i\rangle\langle i|n_i-\sum_{i,j(i\neq j)}\underline{B}^{\,ij}|i\rangle\langle j|\ .\end{aligned} \tag{2.16}$$

Our aim is to find configuration-averaged $\underline{T}^{\,ij}$, which by the augmented-space theorem, is given by

$$\langle\underline{T}^{\,ij}\rangle=\langle i,F|\underline{\tilde{A}}^{\,-1}|j,F\rangle\ , \tag{2.17}$$

where

$$\begin{aligned}\underline{\tilde{A}}=&\,\underline{C}^{\,B}\sum_i|i\rangle\langle i|\otimes\underline{I}+\delta\underline{C}\sum_i|i\rangle\langle i|\otimes\underline{M}^{(i)}\\ &-\sum_{i,j(i\neq j)}\underline{B}^{\,ij}|i\rangle\langle j|\otimes\underline{I}\ .\end{aligned} \tag{2.18}$$

In Eq. (2.18) $\underline{I}$ and $\underline{M}^{(i)}$ are operators in the configuration space Φ. Now we partition the augmented space ψ into subspaces labeled by I and II; the subspace I is spanned by $\{|i,F_s\rangle\}$, $i\in\mathcal{C}$, where $\mathcal{C}$ is the chosen cluster and $\{|F_s\rangle\}$ span the configuration space of the cluster. For a cluster of size m, the subspace I is of rank $m\times 2^m$. The crucial mean-field approximation now involves replacing the conjugate space II by an effective medium. Thus the subspace II has only one configuration, namely, the ground state $|F\rangle$, and hence, is spanned by $\{|j,F\rangle\}$, $j\in\mathcal{C}'$, where $\mathcal{C}'$ is the complement of the cluster $\mathcal{C}$ and is of rank $N-m$.

Since we need the $\langle i,F|\ldots|j,F\rangle$ element $(i,j\in\mathcal{C})$ of $\tilde{\underline{A}}^{-1}$ in Eq. (2.17), we partition $\tilde{\underline{A}}$ as follows:

$$\tilde{\underline{A}}=\begin{bmatrix}\underline{A}_I & \underline{A}'\\ \underline{A}'^T & \underline{A}_{\mathrm{II}}\end{bmatrix}, \tag{2.19}$$

where $\underline{A}_{\mathrm{I}}$ is in the subspace I and $\underline{A}_{\mathrm{II}}$ is in the subspace II. By partition theorem, we get the inverse of $\tilde{\underline{A}}$ in subspace I as

$$[\tilde{\underline{A}}^{-1}]_{\mathrm{I}}=(\underline{A}_{\mathrm{I}}-\underline{A}'\underline{A}_{\mathrm{II}}^{-1}\underline{A}'^T)^{-1}=\hat{\underline{A}}^{-1}\,. \tag{2.20}$$

The four constituent matrices of $\tilde{\underline{A}}$ are given by

$$\begin{aligned}\underline{A}_{\mathrm{I}}=\underline{C}^B\sum_{i\in\mathcal{C}}|i\rangle\langle i|\otimes\sum_{F_s\in\Phi}|F_s\rangle\langle F_s|\\ +\delta\underline{C}\sum_{i\in\mathcal{C}}|i\rangle\langle i|\otimes\underline{M}^{(i)}\\ -\sum_{\substack{i,j\in\mathcal{C}\\(i\neq j)}}\underline{B}^{ij}|i\rangle\langle j|\otimes\sum_{F_s\in\Phi}|F_s\rangle\langle F_s|\,,\end{aligned} \tag{2.21}$$

$$\begin{aligned}\underline{A}_{\mathrm{II}}=\Bigg[&\underline{C}_{\mathrm{eff}}\sum_{k\in\mathcal{C}'}|k\rangle\langle k|-\sum_{\substack{k,l\in\mathcal{C}'\\(k\neq l)}}\underline{b}^{kl}|k\rangle\langle l|\\ &-\sum_{\substack{k,l\in\mathcal{C}'\\(k\neq l)}}\underline{B}^{kl}|k\rangle\langle l|\Bigg]\otimes|F\rangle\langle F|\,,\end{aligned} \tag{2.22}$$

$$\begin{aligned}\underline{A}'=-&\left[\sum_{i\in\mathcal{C}}\sum_{k\in\mathcal{C}'}\underline{b}^{ik}|i\rangle\langle k|+\sum_{i\in\mathcal{C}}\sum_{k\in\mathcal{C}'}\underline{B}^{ik}|i\rangle\langle k|\right]\\ &\otimes\sum_{F_s\in\Phi}|F_s\rangle\langle F|\,,\end{aligned} \tag{2.23}$$

and $\underline{A}'^T$ is the transpose of $\underline{A}'$. In Eqs. (2.22) and (2.23), $\underline{b}^{kl}$ are the off-diagonal corrections in $\underline{C}$, the diagonal corrections already contained in $\underline{C}_{\mathrm{eff}}$. Note that $\underline{A}_{\mathrm{I}}$ does not contain $\underline{b}^{ij}$, because subspace I contains the real atoms and their configurations, while $\underline{A}_{\mathrm{II}}$ has these off-diagonal corrections, because subspace II contains only effective atoms. This partitioning of the augmented space into subspaces I and II is different from the physical partition of the lattice into nonoverlapping clusters of the Tsukada scheme.[8] In the present scheme, the subspaces I and II are interacting and, therefore, the operator $\underline{A}'$, which connects the subspaces I and II, must contain the off-diagonal corrections $\underline{b}^{ik}$, in order to include correlated scattering between a site inside the cluster and site outside the cluster.[21] This ensures that the CCPA preserves the translational invariance of the effective medium. Removing $\underline{b}^{ik}$ from $\underline{A}'$ in Eq. (2.23) will lead to the old Tsukada scheme,[8] which is not the same as our CCPA. In general, $\underline{b}^{kl}$ will not be zero in KKR-CCPA. However, for a one-atom cluster, these terms vanish, thus reducing to the correct KKR-CPA limit. For convenience, we add $\underline{b}^{kl}$ to $\underline{B}^{kl}$ (which are also off-diagonal in site indices) and define $\underline{B}^{kl}_{\mathrm{eff}}$ as

$$\underline{B}^{kl}_{\mathrm{eff}}=\underline{B}^{kl}+\underline{b}^{kl}\,. \tag{2.24}$$

Thus Eqs. (2.22) and (2.23) can now be written as

$$\begin{aligned}\underline{A}_{\mathrm{II}}=&\left[\underline{C}_{\mathrm{eff}}\sum_{k\in\mathcal{C}'}|k\rangle\langle k|-\sum_{\substack{k,l\in\mathcal{C}'\\(k\neq l)}}\underline{B}^{kl}_{\mathrm{eff}}|k\rangle\langle l|\right]\\ &\otimes|F\rangle\langle F|\end{aligned} \tag{2.25}$$

and

$$\underline{A}'=-\left[\sum_{i\in\mathcal{C}}\sum_{k\in\mathcal{C}'}\underline{B}^{ik}_{\mathrm{eff}}|i\rangle\langle k|\right]\otimes\sum_{F_s\in\Phi}|F_s\rangle\langle F|\,. \tag{2.26}$$

The elements of $\hat{\underline{A}}$ in Eq. (2.20) can be found if we can evaluate the triple product $(\underline{A}'\underline{A}_{\mathrm{II}}^{-1}\underline{A}'^T)$. Since $\underline{A}_{\mathrm{II}}$ is the matrix in the effective medium with the cluster $\mathcal{C}$ removed, we have

$$\underline{A}_{\mathrm{II}}^{-1}=\underline{T}^{(\mathcal{C})}_{\mathrm{eff}}\,. \tag{2.27}$$

The superscript $\mathcal{C}$ inside the parentheses indicates that $\underline{T}^{(\mathcal{C})}_{\mathrm{eff}}$ is the path operator matrix of the effective medium with the cluster removed from the medium. Though it is not possible to calculate this quantity, we show in Appendix A that it can be eliminated completely from the computational procedure. From Eqs. (2.25), (2.26), and (2.27) we get

$$\begin{aligned}\underline{A}'\underline{A}_{\mathrm{II}}^{-1}\underline{A}'^T&=\sum_{i,j\in\mathcal{C}}\sum_{k,l\in\mathcal{C}'}\underline{B}^{ik}_{\mathrm{eff}}\underline{T}^{(\mathcal{C})kl}_{\mathrm{eff}}\underline{B}^{lj}_{\mathrm{eff}}|i\rangle\langle j|\\ &\qquad\otimes\sum_{F_s\in\Phi}|F_s\rangle\langle F_s|\\ &=\sum_{i,j\in\mathcal{C}}\underline{\xi}^{ij}_{\mathcal{C}}|i\rangle\langle j|\otimes\sum_{F_s\in\Phi}|F_s\rangle\langle F_s|\,,\end{aligned}$$

where

$$\underline{\xi}^{ij}_{\mathcal{C}}=\sum_{k,l\in\mathcal{C}'}\underline{B}^{ik}_{\mathrm{eff}}\underline{T}^{(\mathcal{C})kl}_{\mathrm{eff}}\underline{B}^{lj}_{\mathrm{eff}}\quad\text{for } i,j\in\mathcal{C}\,. \tag{2.28}$$

It is clear from Eq. (2.28) that the matrix $(\underline{A}'\underline{A}_{\mathrm{II}}^{-1}\underline{A}'^T)$ is diagonal in the configuration space Φ. The off-diagonal parts in $\hat{\underline{A}}$ thus come from $\underline{A}_{\mathrm{I}}$ only. From Eqs. (2.20), (2.21), and (2.28) we get

$$\begin{aligned}\hat{\underline{A}}=&\left[\sum_{i\in\mathcal{C}}(\underline{C}^B-\underline{\xi}^{ii}_{\mathcal{C}})|i\rangle\langle i|-\sum_{\substack{i,j\in\mathcal{C}\\(i\neq j)}}(\underline{B}^{ij}+\underline{\xi}^{ij}_{\mathcal{C}})|i\rangle\langle j|\right]\\ &\otimes\sum_{F_s\in\Phi}|F_s\rangle\langle F_s|+\delta\underline{C}\sum_{i\in\mathcal{C}}|i\rangle\langle i|\otimes\underline{M}^{(i)}\,.\end{aligned} \tag{2.29}$$

We now partition $\hat{\underline{A}}$ as follows:

$$\hat{\underline{A}}=\begin{bmatrix}\underline{A}_1 & \underline{A}_{12}\\ \underline{A}_{21} & \underline{A}_2\end{bmatrix}, \tag{2.30}$$

where $\underline{A}_1$ is in the subspace 1 spanned by $|i,F\rangle$, $i\in\mathcal{C}$ and is of rank m. The subspace 2 is the complement of subspace 1 and has rank $m \times (2^m - 1)$. The inverse of $\underline{\hat{A}}$ in subspace 1 is then given by

$$[\underline{\hat{A}}^{-1}]_1 = (\underline{A}_1 - \underline{A}_{12}\underline{A}_2^{-1}\underline{A}_{21})^{-1} . \tag{2.31}$$

Since the ranks of the matrices $\underline{A}_1$, $\underline{A}_{12}$, $\underline{A}_{21}$, and $\underline{A}_2$ are small, it is not difficult to find the matrix elements in Eq. (2.31). In Appendix A we show that these can be found analytically for small clusters.

The matrix $\underline{A}_1$ can be obtained from Eq. (2.29) as

$$\underline{A}_1 = \sum_{i \in \mathcal{C}} (\underline{\bar{C}} - \underline{\xi}_{\mathcal{C}}^{ii})|i\rangle\langle i| - \sum_{\substack{i,j \in \mathcal{C} \\ (i \neq j)}} (\underline{B}^{ij} + \underline{\xi}_{\mathcal{C}}^{ij})|i\rangle\langle j| , \tag{2.32}$$

where

$$\underline{\bar{C}} = x\underline{C}^A + y\underline{C}^B .$$

From Eq. (2.17) we get

$$\langle \underline{T}^{ij} \rangle = \langle i|(\underline{A}_1 - \underline{A}_{12}\underline{A}_2^{-1}\underline{A}_{21})^{-1}|j\rangle \quad \text{for } i,j \in \mathcal{C} . \tag{2.33}$$

For the translationally invariant effective medium, Eq. (2.16) can be rewritten as

$$\underline{A}_{\text{eff}} = \underline{C}_{\text{eff}} \sum_i |i\rangle\langle i| - \sum_{\substack{i,j \\ (i \neq j)}} \underline{B}_{\text{eff}}^{ij}|i\rangle\langle j| . \tag{2.34}$$

We get the effective path operators, for the sites inside the cluster, from Eq. (2.34) by the partitioning technique as

$$\underline{T}_{\text{eff}}^{ij} = \left\langle i \left| \left[\sum_{k \in \mathcal{C}} (\underline{C}_{\text{eff}} - \underline{\xi}_{\mathcal{C}}^{kk})|k\rangle\langle k| - \sum_{\substack{k,l \in \mathcal{C} \\ (k \neq l)}} (\underline{B}_{\text{eff}}^{kl} + \underline{\xi}_{\mathcal{C}}^{kl})|k\rangle\langle l| \right]^{-1} \right| j \right\rangle . \tag{2.35}$$

The self-consistency condition $\langle \underline{T}^{ij} \rangle = \underline{T}_{\text{eff}}^{ij}$ implies that

$$\underline{A}_1 - \underline{A}_{12}\underline{A}_2^{-1}\underline{A}_{21} = \sum_{i \in \mathcal{C}} (\underline{C}_{\text{eff}} - \underline{\xi}_{\mathcal{C}}^{ii})|i\rangle\langle i| - \sum_{\substack{i,j \in \mathcal{C} \\ (i \neq j)}} (\underline{B}_{\text{eff}}^{ij} + \underline{\xi}_{\mathcal{C}}^{ij})|i\rangle\langle j| . \tag{2.36}$$

The KKR-CCPA equations follow directly from Eq. (2.36) as

$$\underline{C}_{\text{eff}} = \underline{\bar{C}} - \langle i|\underline{A}_{12}\underline{A}_2^{-1}\underline{A}_{21}|i\rangle , \tag{2.37a}$$

$$\underline{b}^{ij} = \langle i|\underline{A}_{12}\underline{A}_2^{-1}\underline{A}_{21}|j\rangle \quad \text{for } ij(i \neq j) \in \mathcal{C} . \tag{2.37b}$$

The path operator matrices can be calculated by the usual **k**-space integration over the first Brillouin zone as

$$\underline{T}_{\text{eff}}^{nm} = \frac{\Omega}{8\pi^3} \int_{\text{BZ}} [\underline{C}_{\text{eff}} - \underline{B}_{\text{eff}}(\mathbf{k},E)]^{-1} \exp(-i\mathbf{k}\cdot\mathbf{R}_{nm}) d\mathbf{k} , \tag{2.38}$$

where $\underline{B}_{\text{eff}}(\mathbf{k},E)$ is the Fourier transform of $\underline{B}_{\text{eff}}^{nm}$, i.e.,

$$\begin{aligned} \underline{B}_{\text{eff}}(\mathbf{k},E) &= \sum_n \underline{B}_{\text{eff}}^{0n} \exp(i\mathbf{k}\cdot\mathbf{R}_{0n}) \\ &= \underline{B}(\mathbf{k},E) + \sum_{i \in \mathcal{C}} \underline{b}^{0i} \exp(i\mathbf{k}\cdot\mathbf{R}_{0i}) . \end{aligned} \tag{2.39}$$

Note that

$$\underline{b}^{ji} = (\underline{b}^{ij})^T ,$$

and therefore we need to solve Eq. (2.37b) for $j > i$ only. This reduces the number of self-consistent coupled equations in Eqs. (2.37a) and (2.37b) to $m(m-1)/2+1$. This number can be further reduced by exploiting the symmetry of the cluster. Note that all these equations involve matrices of rank $(l+1)^2$, where l is the maximum number of angular momentum states used in evaluating the phase shifts. Therefore, with modern computing facilities, solving KKR-CCPA equations for a five-site cluster (for which there are 11 coupled equations) will not be difficult at all.

A cluster consisting of a central site and its shell of nearest neighbors should be the ideal choice but it will be computationally demanding and so we propose an alternative, though approximate method. One can take a two-atom cluster consisting of the central site (site 0) and one of its nearest neighbors (say, site 1). The KKR-CCPA equations for a two-atom cluster are given in Appendix A. By solving equations, one can obtain $\underline{C}_{\text{eff}}$ and $\underline{b}^{01}$. Then $\underline{b}^{0m}$, for the rest of the nearest neighbors, can be found by rotational symmetry, since $\underline{b}^{ij}$ will transform like $\underline{B}^{ij}$. These $\underline{b}^{0i}$ can then be used in Eq. (2.39).

C. The configuration-averaged Green's function

The configuration-averaged Green's functions for site-diagonal (SD) and non-site-diagonal (NSD) cases can be written from Eq. (2.11) as

$$\langle \underline{G}_{\text{SD}}(\mathbf{r},\mathbf{r}';E) \rangle = \text{Tr}\langle \underline{F}^i(\mathbf{r}_i,\mathbf{r}_i')\underline{T}^{ii} \rangle - \sum_L \langle \underline{Z}_L^i(\mathbf{r}_i)\underline{J}_L^i(\mathbf{r}_i') \rangle$$

and

$$\langle \underline{G}_{\text{NSD}}(\mathbf{r},\mathbf{r}';E) \rangle = \text{Tr}\langle \underline{F}^{ij}(\mathbf{r}_i,\mathbf{r}_j')\underline{T}^{ij} \rangle , \tag{2.40}$$

where the trace is over the angular momentum indices only and

$$\begin{aligned} \underline{F}_{LL'}^i(\mathbf{r}_i,\mathbf{r}_i') &= \underline{Z}_L^i(\mathbf{r}_i)\underline{Z}_{L'}^i(\mathbf{r}_i') , \\ \underline{F}_{LL'}^{ij}(\mathbf{r}_i,\mathbf{r}_j') &= \underline{Z}_L^j(\mathbf{r}_j')\underline{Z}_{L'}^i(\mathbf{r}_i) . \end{aligned} \tag{2.41}$$

To find the joint averages in Eq. (2.40) we adopt the method of Ref. 30. In this method, a single atom is treated exactly, while the rest is effective medium. Equation (2.40) can now be written as

$$\langle \underline{G}_{\mathrm{SD}}(\mathbf{r},\mathbf{r}';E)\rangle = \mathrm{Tr}[x\underline{F}^{A}(\mathbf{r}_i,\mathbf{r}_i')\langle \underline{T}^{ii}\rangle_A + y\underline{F}^{B}(\mathbf{r}_i,\mathbf{r}_i')\langle \underline{T}^{ii}\rangle_B] - \sum_L [x\underline{Z}_L^A(\mathbf{r}_i)\underline{J}_L^A(\mathbf{r}_i') + y\underline{Z}_L^B(\mathbf{r}_i)\underline{J}_L^B(\mathbf{r}_i')]$$

and

$$\langle \underline{G}_{\mathrm{NSD}}(\mathbf{r},\mathbf{r}';E)\rangle = \mathrm{Tr}\{x^2\underline{F}^{AA}(\mathbf{r}_i,\mathbf{r}_j')\langle \underline{T}^{ij}\rangle_{AA} + y^2\underline{F}^{BB}(\mathbf{r}_i,\mathbf{r}_j')\langle \underline{T}^{ij}\rangle_{BB} + xy[F^{AB}(\mathbf{r}_i,\mathbf{r}_j')\langle \underline{T}^{ij}\rangle_{AB} + \underline{F}^{BA}(\mathbf{r}_i,\mathbf{r}_j')\langle \underline{T}^{ij}\rangle_{BA}]\}\ , \tag{2.42}$$

where $\langle \underline{T}^{ii}\rangle_\alpha$ and $\langle \underline{T}^{ij}\rangle_{\alpha\beta}(\alpha,\beta = A$ or $B)$ are the restricted averages. To find these restricted averages, we embed a single impurity in the effective medium. Now we recall that, in the determination of the effective medium, the off-diagonal term between real and effective atoms is taken as $\underline{B}_{\mathrm{eff}}^{ij}$. Therefore, to be consistent in the prescription of these off-diagonal terms, in the present case also, we take them to be $\underline{B}_{\mathrm{eff}}^{ij}$. In Appendix C, we discuss the effect of change in the off-diagonal terms between real and effective atoms on the DOS. In the present prescription, the restricted averages can be found by a simple partitioning technique, similar to Ref. 30, to give

$$\langle \underline{T}^{ii}\rangle_\alpha = \underline{D}^{\alpha}\underline{T}_{\mathrm{eff}}^{ii} \tag{2.43a}$$

and

$$\langle \underline{T}^{ij}\rangle_{\alpha\beta} = \underline{D}^{\alpha}\underline{T}_{\mathrm{eff}}^{ij}[\underline{I} - (\underline{C}^{\beta} - \underline{C}_{\mathrm{eff}})D^{\beta}\underline{T}_{\mathrm{eff}}^{ji}(\underline{C}^{\alpha} - \underline{C}_{\mathrm{eff}}) \times \underline{D}^{\alpha}\underline{T}_{\mathrm{eff}}^{ij}]^{-1}\underline{D}^{\beta}\ , \tag{2.43b}$$

where

$$\underline{D}^{\alpha} = [\underline{I} + (\underline{C}^{\alpha} - \underline{C}_{\mathrm{eff}})\underline{T}_{\mathrm{eff}}^{00}]^{-1}\ . \tag{2.44}$$

The total and component DOS's per atom are obtained by integrating the SD Green's function over the unit cell,

$$n(E) = -\frac{1}{\pi}\mathrm{Tr}\,\mathrm{Im}(x\underline{F}^{A}\underline{D}^{A} + y\underline{F}^{B}\underline{D}^{B})\underline{T}_{\mathrm{eff}}^{00}\ , \tag{2.45}$$

$$n^{\alpha}(E) = -\frac{1}{\pi}\mathrm{Tr}\,\mathrm{Im}\underline{F}^{\alpha}\underline{D}^{\alpha}\underline{T}_{\mathrm{eff}}^{00}\ , \tag{2.46}$$

where

$$\underline{F}^{\alpha} = \int_{\Omega}\underline{F}^{\alpha}(\mathbf{r}_n,\mathbf{r}_n)d\mathbf{r}_n\ . \tag{2.47}$$

For the charge self-consistency within the local-density approximation of the density-functional theory, one needs the component charge densities. To find the component charge densities we embed a single atom in the effective medium.[35] The average charge density $\rho(\mathbf{r})$ and component charge density $\rho^{(\alpha)}(\mathbf{r})$ $(\alpha = A,B)$ are given by

$$\rho(\mathbf{r}) = -\frac{1}{\pi}\mathrm{Tr}\,\mathrm{Im}\int_{-\infty}^{E_F}[x\underline{F}^{A}(\mathbf{r},\mathbf{r})\underline{D}^{A} + y\underline{F}^{B}(\mathbf{r},\mathbf{r})\underline{D}^{B}] \times \underline{T}_{\mathrm{eff}}^{00}dE\ , \tag{2.48}$$

$$\rho^{(\alpha)}(\mathbf{r}) = -\frac{1}{\pi}\mathrm{Tr}\,\mathrm{Im}\int_{-\infty}^{E_F}\underline{F}^{\alpha}(\mathbf{r},\mathbf{r})\underline{D}^{\alpha}\underline{T}_{\mathrm{eff}}^{00}dE\ . \tag{2.49}$$

One can construct the potentials $v^{(\alpha)}(\mathbf{r})$ from $\rho^{(\alpha)}(\mathbf{r})$ in the local-density approximation and thus can achieve charge self-consistency.

For a single impurity of type α in the effective medium, the local DOS on the impurity site can be obtained from Eq. (2.46). If we embed two impurities of type α and β on the sites i and j, respectively, the local DOS on the respective sites will be given by

$$n_2^{(\alpha)}(E) = -\frac{1}{\pi}\mathrm{Tr}\,\mathrm{Im}[\underline{F}^{\alpha}\langle \underline{T}^{ij}\rangle_{ij}]$$

and

$$n_2^{(\beta)}(E) = -\frac{1}{\pi}\mathrm{Tr}\,\mathrm{Im}[\underline{F}^{\beta}\langle \underline{T}^{jj}\rangle_{ij}]\ . \tag{2.50}$$

Hence we need only to find the path operator matrices $\langle \underline{T}^{ii}\rangle_{ij}$ and $\langle \underline{T}^{jj}\rangle_{ij}$. It is straightforward to obtain these matrices by the partitioning technique. The real space is divided into two subspaces; one for the impurity sites and the other for the rest effective medium. Then by simple matrix algebra one easily gets

$$\langle \underline{T}^{ii}\rangle_{ij} = \{[\underline{T}_{\mathrm{eff}}^{00} - \underline{T}_{\mathrm{eff}}^{ij}(\underline{C}^{\beta} - \underline{C}_{\mathrm{eff}})\underline{D}^{\beta}\underline{T}_{\mathrm{eff}}^{ji}]^{-1} + (\underline{C}^{\alpha} - \underline{C}_{\mathrm{eff}})\}^{-1}$$

and

$$\langle \underline{T}^{jj}\rangle_{ij} = \{[\underline{T}_{\mathrm{eff}}^{00} - \underline{T}_{\mathrm{eff}}^{ji}(\underline{C}^{\alpha} - \underline{C}_{\mathrm{eff}})\underline{D}^{\alpha}\underline{T}_{\mathrm{eff}}^{ij}]^{-1} + (\underline{C}^{\beta} - \underline{C}_{\mathrm{eff}})\}^{-1}\ . \tag{2.51}$$

Equations (2.46)–(2.51) are rather general and can be used to calculate local DOS and charge densities for a single impurity or two impurities of foreign kind in the effective medium.

III. RESULTS AND DISCUSSION

In this section we present the results of our calculations of DOS for a one-dimensional muffin-tin alloy. All the relevant equations for this model are given in Appendix B. The lattice parameters ($a = 6.00$ a.u.) and the muffin-tin radii ($r_m = 2.25$ a.u.) of the two components of the alloy are identical. The depths of the two constituent potentials are $V_A = -0.3$ Ry and $V_B = -0.5$ Ry. The DOS for the two pure systems is shown in Fig. 1, which shows peaks at band edges, characteristics of the one-dimensional model. For the KKR-CCPA calculations we have taken a two-atom cluster. In Fig. 2 we show the results of our calculations in the low concentration ($x = 0.1$) limit. Figure 2(a) shows the KKR-CPA and KKR-CCPA DOS's. We note that, in the first majority band, there is no apparent difference in the KKR-CPA and KKR-CCPA results. However, in the impurity band we observe a shoulder in the KKR-CCPA DOS around $E = -0.16$ Ry and a peak at $E = -0.12$ Ry, in contrast to a smooth KKR-CPA impurity band centered around $E = -0.14$ Ry. The extra structures in the KKR-CCPA

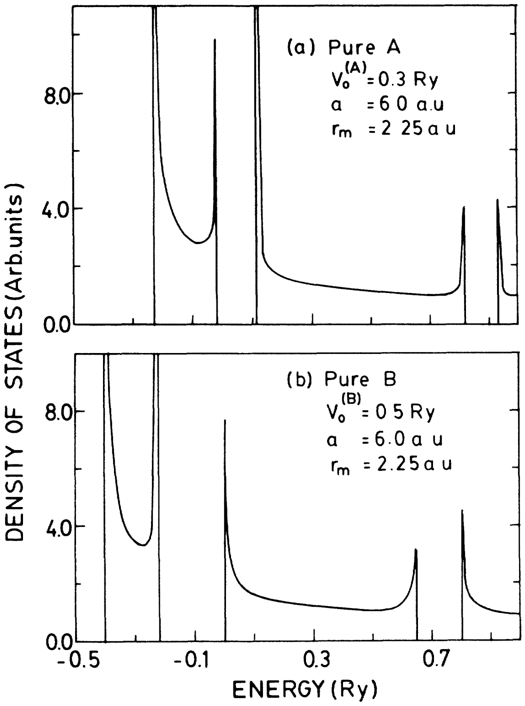

FIG. 1. DOS for the one-dimensional systems of potential depths (a) $V_A = 0.3$ Ry and (b) $V_B = 0.5$ Ry.

DOS seem to arise due to correlated scattering from two-atom clusters. This becomes clear by a close inspection of the local DOS on impurities for a two-impurity cluster embedded in the KKR-CPA medium, as shown in Figs. (2b) and (2c). If we look at the local DOS on the A-type impurity of an AA-type cluster, as shown in Fig. 2(b), we observe that its impurity band is almost identical to that of the KKR-CCPA DOS, thus explaining the above-mentioned structure. We also observe a peak at $E = -0.13$ Ry in the local DOS on the A-type impurity of an AB-type cluster, as shown in Fig. 2(c), which is close to the peak at $E = -0.12$ Ry in the KKR-CCPA DOS. Also, a small but observable structure at $E = 0.06$ Ry in the KKR-CCPA DOS is very close to the two kinks around $E = 0.04$ Ry in the local DOS on both A-type and B-type impurities of an AB-type cluster, as shown in Fig. 2(c). In Fig. 2(d) we show the local DOS on A-type impurities in a pure B medium. We observe that the two-impurity levels at $E = -0.19$ and -0.10 Ry are close enough to the structures in the minority band of the KKR-CCPA DOS. This further supports our assertion that these structures arise from two-impurity scattering.

Figure 3 shows the results for a concentrated alloy ($x = 0.5$). As shown in Fig. 3(a), the KKR-CPA gives a rather smooth DOS besides a peak in each band while the KKR-CCPA, once again gives few extra structures in all the bands. The KKR-CPA peaks at $E = -0.38$, -0.21, and 0.04 Ry almost coincide with the major KKR-CCPA peaks at $E = -0.39$, -0.21, and 0.04 Ry. Besides these major peaks, we observe some more peaks at $E = -0.35$,

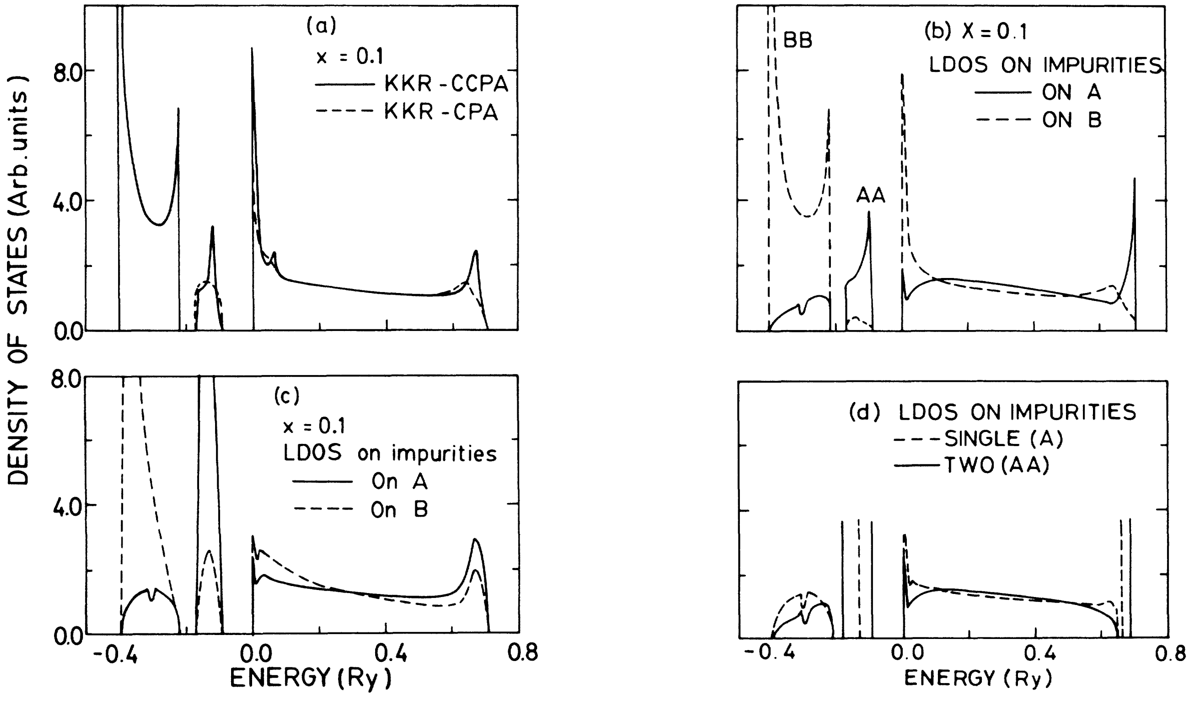

FIG. 2. (a) KKR-CPA (dashed line) and KKR-CCPA (solid line) DOS's for the alloy with concentration $x = 0.1$. (b) Local DOS on the impurity site for a cluster of two impurities of AA (solid line) and BB (dashed line) type embedded in the KKR-CPA medium for $x = 0.1$. (c) Local DOS on the impurity site of A (solid line) and B (dashed line) type of an AB-type cluster embedded in the KKR-CPA medium for $x = 0.1$. (d) Local DOS on the impurity site for a single (dashed line) and two (solid line) impurities of type A embedded in the pure B medium.

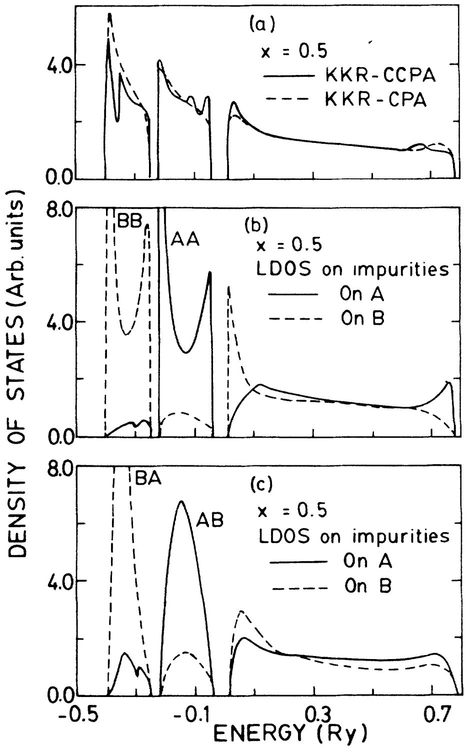

FIG. 3. (a) KKR-CPA (dashed line) and KKR-CCPA (solid line) DOS's for the alloy with concentration $x = 0.5$. (b) Local DOS on the impurity site for a cluster of two impurities of AA (solid line) and BB (dashed line) type embedded in the KKR-CPA medium for $x = 0.5$. (c) Local DOS on the impurity site of A (solid line) and B (dashed line) type of a cluster of AB type embedded in the KKR-CPA medium for $x = 0.5$.

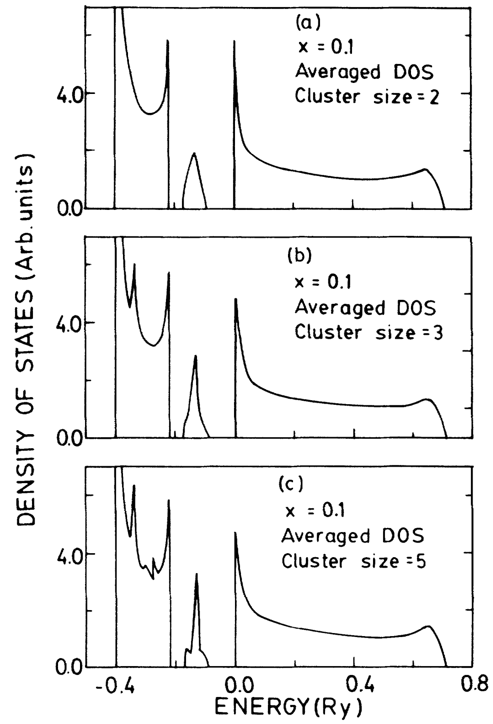

FIG. 4. Averaged DOS on the central site of a cluster of (a) two atoms, (b) three atoms, and (c) five atoms, embedded in the KKR-CPA medium for $x = 0.1$.

−0.11, and −0.06 Ry, in the KKR-CCPA DOS. As in the case of $x = 0.1$, these extra structures in the KKR-CCPA DOS are very close to the structures in the local DOS on the impurities of a two-impurity cluster embedded in the KKR-CPA medium. In Figs. 3(b) and 3(c) we show, respectively, the local DOS's on the impurities of a cluster of two like and unlike impurities embedded in the KKR-CPA medium. We observe that the KKR-CCPA peak at $E = -0.35$ Ry is exactly at the position of the peak in the local DOS on a B-type impurity of an AB-type cluster, as shown in Fig. 3(c). Thus the KKR-CCPA peak at $E = -0.35$ Ry is identified as due to the B-type atoms. The second extra peak at $E = -0.11$ Ry is close to the peak in the local DOS on an A-type impurity of an AB-type cluster, which is at $E = -0.14$ Ry. The third extra peak at $E = -0.06$ Ry can be identified as due to the A-type atoms as it is very close to a peak in the local DOS on an A-type impurity of an AA-type cluster at $E = -0.05$ Ry as shown in Fig. 3(b).

We have also compared our KKR-CCPA results with some calculations obtained by using the embedded cluster approach of Gonis *et al.*[13] We have embedded clusters of two, three, and five atoms in the KKR-CPA medium. The averaged DOS on the central site of the cluster is obtained by calculating the local DOS on the central site for all possible configurations of the cluster and then taking the average. This averaged DOS produces some of the structures of the KKR-CCPA DOS. In Figs. 4(a), 4(b), and 4(c), we show the averaged DOS, for different cluster size, in the low concentration limit ($x = 0.1$). We observe that, for a two-atom cluster, the averaged DOS does not give the structures of the KKR-CCPA DOS.

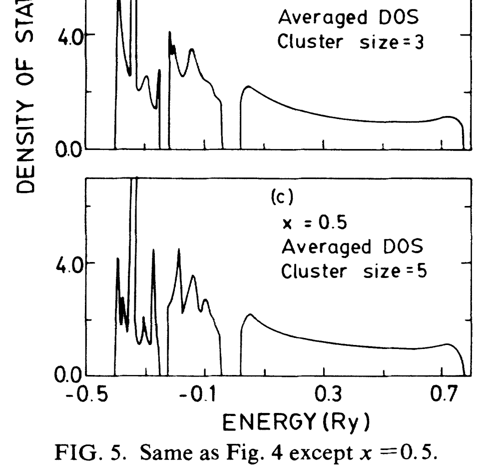

FIG. 5. Same as Fig. 4 except $x = 0.5$.

However, as we increase the cluster size, the structures in the averaged DOS become prominent, and show resemblance to the KKR-CCPA results. For the higher concentration ($x=0.5$) also, the averaged DOS, as shown in Figs. 5(a), 5(b), and 5(c), does reproduce the structures of the KKR-CCPA DOS in Fig. 3(a), which become more prominent with the increase in the cluster size.

IV. CONCLUSION

We have shown that one can go beyond the CPA in the first-principles KKR Green's-function method by effectively combining the ASF with the conventional KKR method. It has been put on the same rigorous footing as KKR-CPA in which one can calculate DOS, component DOS, and charge densities, self-consistently. We have shown that the KKR-CCPA, unlike the KKR-CPA, introduces off-diagonal corrections to the scattering matrices. Our calculations on a model alloy show that the structures in the KKR-CCPA DOS are due to correlated scattering from clusters of atoms in the effective medium.

ACKNOWLEDGMENTS

One of the authors (R.P.) thanks Professor V. Heine for his kind hospitality at the Cavendish Laboratory, U.K., and some helpful discussions. He also acknowledges discussions with Professor A. Bansil, Professor R. Haydock, Professor B. L. Gyorffy, and Dr. R. Benedek. This work was supported by the Department of Science and Technology, New Delhi, India, through Grant No. SP/S2/M-39/87.

APPENDIX A:
KKR-CCPA FOR ONE- AND TWO-ATOM CLUSTERS

For a one-atom cluster (the 0th site) the configuration space ϕ_0 is spanned by $|f_0^{(0)}\rangle$ and $|f_1^{(0)}\rangle$. Then Eq. (2.21) reduces to

$$\underline{A}_{\mathrm{I}}=\begin{bmatrix}\bar{\underline{C}} & \underline{\omega}\\ \underline{\omega} & \tilde{\underline{C}}\end{bmatrix}, \tag{A1}$$

where

$$\tilde{\underline{C}}=y\underline{C}^{A}+x\underline{C}^{B}$$

and

$$\underline{\omega}=(xy)^{1/2}(\underline{C}^{A}-\underline{C}^{B}) . \tag{A2}$$

Rewriting Eqs. (2.28) and (2.29) for this case we get

$$\underline{\xi}_1^{00}=\sum_{j,k\neq 0}\underline{B}_{\mathrm{eff}}^{0j}\underline{T}_{\mathrm{eff}}^{(0)jk}\underline{B}_{\mathrm{eff}}^{k0} \tag{A3}$$

and

$$\hat{\underline{A}}=\begin{bmatrix}\bar{\underline{C}}-\underline{\xi}_1^{00} & \underline{\omega}\\ \underline{\omega} & \tilde{\underline{C}}-\underline{\xi}_1^{00}\end{bmatrix} . \tag{A4}$$

The matrices $\underline{A}_{\mathrm{I}}$ and $\hat{\underline{A}}$ are in a space spanned by $|0,f_0^{(0)}\rangle$ and $|0,f_1^{(0)}\rangle$. Now for the effective medium we have

$$\begin{aligned}\underline{T}_{\mathrm{eff}}^{00}&=\Big[\underline{C}_{\mathrm{eff}}-\sum_{j,k\neq 0}\underline{B}_{\mathrm{eff}}^{0j}\underline{T}_{\mathrm{eff}}^{(0)jk}\underline{B}_{\mathrm{eff}}^{k0}\Big]^{-1}\\ &=(\underline{C}_{\mathrm{eff}}-\underline{\xi}_1^{00})^{-1}\end{aligned} \tag{A5}$$

and thus

$$\underline{\xi}_1^{00}=\underline{C}_{\mathrm{eff}}-(\underline{T}_{\mathrm{eff}}^{00})^{-1} . \tag{A6}$$

By the augmented-space theorem we have

$$\begin{aligned}\underline{T}_{\mathrm{eff}}^{00}&=\langle 0,f_0^{(0)}|\hat{\underline{A}}^{-1}|0,f_0^{(0)}\rangle\\ &=[\bar{\underline{C}}-\underline{\xi}_1^{00}-\underline{\omega}(\tilde{\underline{C}}-\underline{\xi}_1^{00})^{-1}\underline{\omega}]^{-1} .\end{aligned} \tag{A7}$$

Comparing (A5) and (A7) we get the KKR-CPA equation

$$\begin{aligned}\underline{C}_{\mathrm{eff}}&=\bar{\underline{C}}-\underline{\omega}(\tilde{\underline{C}}-\underline{\xi}_1^{00})^{-1}\underline{\omega}\\ &=\bar{\underline{C}}-\underline{\omega}[\tilde{\underline{C}}-\underline{C}_{\mathrm{eff}}+(\underline{T}_{\mathrm{eff}}^{00})^{-1}]^{-1}\omega\end{aligned}$$

which readily reduces to the familiar form

$$\underline{C}_{\mathrm{eff}}=\bar{\underline{C}}+(\underline{C}^{A}-\underline{C}_{\mathrm{eff}})\underline{T}_{\mathrm{eff}}^{00}(\underline{C}^{B}-\underline{C}_{\mathrm{eff}}) . \tag{A8}$$

For a two-atom cluster of sites 0 and 1, the configuration space is spanned by four vectors, which are $|F\rangle=|f_0^{(0)}f_0^{(1)}\rangle$, $|F_1\rangle=|f_0^{(0)}f_1^{(1)}\rangle$, $|F_0\rangle=|f_1^{(0)}f_0^{(1)}\rangle$, and $|F_{01}\rangle=|f_1^{(0)}f_1^{(1)}\rangle$. The augmented space is spanned by eight bases $|i,\mathcal{F}\rangle$, $i=0,1$ and $\mathcal{F}=F, F_0, F_1$, and F_{01}.

For this case, Eq. (2.28) reduces to

$$\underline{\xi}_2^{ij}=\sum_{k,l\neq 0,1}\underline{B}_{\mathrm{eff}}^{ik}\underline{T}_{\mathrm{eff}}^{(0,1)kl}\underline{B}_{\mathrm{eff}}^{lj}\ \text{ for } i,j=0,1 . \tag{A9}$$

It is evident that $\underline{\xi}_2^{00}=\underline{\xi}_2^{11}$. By partitioning the effective medium to get the path operators for the sites inside the cluster, we get

$$\begin{bmatrix}\underline{T}_{\mathrm{eff}}^{00} & \underline{T}_{\mathrm{eff}}^{01}\\ \underline{T}_{\mathrm{eff}}^{10} & \underline{T}_{\mathrm{eff}}^{11}\end{bmatrix}=\left[\begin{bmatrix}\underline{C}_{\mathrm{eff}} & -\underline{B}_{\mathrm{eff}}^{01}\\ -\underline{B}_{\mathrm{eff}}^{10} & \underline{C}_{\mathrm{eff}}\end{bmatrix}-\begin{bmatrix}\underline{\xi}_2^{00} & \underline{\xi}_2^{01}\\ \underline{\xi}_2^{10} & \underline{\xi}_2^{11}\end{bmatrix}\right]^{-1},$$

which gives

$$\begin{aligned}\underline{\xi}_2^{00}&=\underline{C}_{\mathrm{eff}}-[\underline{T}_{\mathrm{eff}}^{00}-\underline{T}_{\mathrm{eff}}^{01}(\underline{T}_{\mathrm{eff}}^{00})^{-1}\underline{T}_{\mathrm{eff}}^{10}]^{-1} ,\\ \underline{\xi}_2^{01}&=-\underline{B}_{\mathrm{eff}}^{01}+[\underline{T}_{\mathrm{eff}}^{00}(\underline{T}_{\mathrm{eff}}^{01})^{-1}\underline{T}_{\mathrm{eff}}^{00}-\underline{T}_{\mathrm{eff}}^{10}]^{-1} ,\\ \underline{\xi}_2^{10}&=-\underline{B}_{\mathrm{eff}}^{10}+[\underline{T}_{\mathrm{eff}}^{00}(\underline{T}_{\mathrm{eff}}^{10})^{-1}\underline{T}_{\mathrm{eff}}^{00}-\underline{T}_{\mathrm{eff}}^{01}]^{-1} .\end{aligned} \tag{A10}$$

Thus with this technique it is possible to eliminate the infinite sum in Eq. (A9) and calculate $\underline{\xi}_2^{ij}$ explicitly in terms of the known effective medium quantities.

Partitioning $\hat{\underline{A}}$ in the scheme of Eq. (2.30) we get

$$\begin{aligned}\underline{A}_1&=\begin{bmatrix}\bar{\underline{C}}-\underline{\xi}_2^{00} & -V^{01}\\ -V^{10} & \bar{\underline{C}}-\underline{\xi}_2^{00}\end{bmatrix},\\ \underline{A}_{12}&=\begin{bmatrix}0 & 0 & 0 & 0 & 0 & \omega\\ \omega & 0 & 0 & 0 & 0 & 0\end{bmatrix},\\ \underline{A}_{21}&=\underline{A}_{12}^{T},\end{aligned} \tag{A11}$$

where

$$V^{ij}=\underline{B}^{ij}+\underline{\xi}_2^{ij}\ \text{ for } i,j=0,1 . \tag{A12}$$

Now the KKR-CCPA equations (2.37a) and (2.37b) reduce to the following two equations:

$$\underline{C}_{\text{eff}}=\bar{\underline{C}}-\langle 0|\underline{A}_{12}\underline{A}_2^{-1}\underline{A}_{21}|0\rangle=\bar{\underline{C}}-\underline{\omega}Q^{00}\underline{\omega}$$

and

$$\underline{b}^{01}=\langle 0|\underline{A}_{12}\underline{A}_2^{-1}\underline{A}_{21}|1\rangle=\underline{\omega}Q^{01}\underline{\omega}\ , \tag{A13}$$

where

$$Q^{00}=R_6^{-1}\ ,$$

$$Q^{01}=R_6^{-1}V^{01}R_5^{-1}\omega R_4^{-1}V^{10}R_3^{-1}\omega R_2^{-1}V^{01}R_1^{-1}\ , \tag{A14}$$

and

$$\begin{aligned}
R_1&=\tilde{\underline{C}}-\underline{\xi}_2^{00}\ ,\\
R_2&=\bar{\underline{C}}-\underline{\xi}_2^{00}-V^{01}R_1^{-1}V^{10}\ ,\\
R_3&=\tilde{\underline{C}}-\underline{\xi}_2^{00}-\underline{\omega}R_2^{-1}\omega\ ,\\
R_4&=\tilde{\underline{C}}-\underline{\xi}_2^{00}-V^{10}R_3^{-1}V^{01}\ ,\\
R_5&=\bar{\underline{C}}-\underline{\xi}_2^{00}-\omega R_4^{-1}\omega\ ,\\
R_6&=\tilde{\underline{C}}-\underline{\xi}_2^{00}-V^{01}R_5^{-1}V^{10}\ .
\end{aligned} \tag{A15}$$

Note that $\underline{C}_{\text{eff}}$ may no longer be diagonal in angular momentum space.

APPENDIX B: ONE-DIMENSIONAL ALLOY MODEL

We consider a one-dimensional alloy of nonoverlapping muffin-tin (MT) potentials described by the Hamiltonian

$$H=-\frac{d^2}{dx^2}+\sum_n v_n(x-na)\ . \tag{B1}$$

In close analogy with the MT model in three dimensions we assume that $v_n(x)$ is symmetric in x and vanishes for $|x|\geq r_m$ (the MT radius), $r_m\leq a/2$ (a is the lattice constant). This one-dimensional model retains many of the features of the three-dimensional MT system.[34] But, in this case, we have only two components of angular momentum ($l=0$ and 1).[34] The SD Green's function for this system is given by

$$\text{Im}\underline{G}(x,x')=\sum_{l,l'}\underline{Z}_l(x)\text{Im}(\underline{T}_{ll'}^{00})\underline{Z}_{l'}(x')\ , \tag{B2}$$

where $\underline{Z}_l(x)$ are the solutions of the Schrödinger equation. The on-the-shell matrix elements of the path operators are given by the integral

$$\underline{T}_{\text{eff}}^{ij}=\frac{a}{2\pi}\int_{-\pi/a}^{\pi/a}dk[\underline{C}_{\text{eff}}-\underline{B}_{\text{eff}}(k,E)]^{-1}\exp[ik(i-j)a]\ , \tag{B3}$$

where $\underline{B}_{\text{eff}}(k,E)$ are given by Eq. (2.39) as

$$\underline{B}_{\text{eff}}(k,E)=\underline{B}(k,E)+\underline{b}^{01}\exp(ika)\ . \tag{B4}$$

$\underline{B}(k,E)$ are the KKR structure functions in one dimension and have explicit expressions.[34] Equation (B3) can be transformed into a contour integration by putting $z=\exp(ika)$:

$$\underline{T}_{\text{eff}}^{ij}=\frac{1}{2\pi i}\oint_C dz\, z^{j-i-l}\frac{g(z)}{\lambda z^4+\delta z^3+\alpha z^2+\beta z+\gamma}\ , \tag{B5}$$

where C is the unit circle centered at $z=0$ and $g(z)$ is a matrix in l space and is given by

$$\begin{aligned}
g_{00}(z)&=[z^2+1-2z\cos(Ka)]\\
&\quad\times(i-K\underline{C}_{11}+K\underline{b}_{11}z)+2z\sin(Ka)\ ,\\
g_{11}(z)&=[z^2+1-2z\cos(Ka)]\\
&\quad\times(i-K\underline{C}_{00}+K\underline{b}_{00}z)+2z\sin(Ka)\ ,\\
g_{01}(z)&=K(\underline{C}_{01}-\underline{b}_{01}z)[z^2+1-2z\cos(Ka)]+z^2-1\ ,\\
g_{10}(z)&=K(\underline{C}_{10}-\underline{b}_{10}z)[z^2+1-2z\cos(Ka)]-z^2+1\ ,
\end{aligned} \tag{B6}$$

and the constants appearing in the denominator of (B5) are

$$\begin{aligned}
\lambda&=E(\underline{b}_{00}\underline{b}_{11}-\underline{b}_{01}\underline{b}_{10})\ ,\\
\delta&=\eta-K(\underline{b}_{01}-\underline{b}_{10})-2\lambda\cos(Ka)\ ,\\
\alpha&=\lambda+\gamma+2K(\underline{C}_{01}-\underline{C}_{10})-2\eta\cos(Ka)\ ,\\
\beta&=2\cos(Ka)[2-\gamma-K(\underline{C}_{01}-\underline{C}_{10})]\\
&\quad+2\sin(Ka)[2i-K(\underline{C}_{00}+\underline{C}_{11})]\\
&\quad+\eta+K(\underline{b}_{01}-\underline{b}_{10})\ ,\\
\gamma&=E(\underline{C}_{00}\underline{C}_{11}-\underline{C}_{01}\underline{C}_{10})\\
&\quad-iK(\underline{C}_{00}+\underline{C}_{11})-K(\underline{C}_{01}-\underline{C}_{10})\ ,\\
\eta&=iK(\underline{b}_{00}+\underline{b}_{11})\\
&\quad-E(\underline{C}_{00}\underline{b}_{11}+\underline{C}_{11}\underline{b}_{00}-\underline{C}_{01}\underline{b}_{10}-\underline{C}_{10}\underline{b}_{01})\ .
\end{aligned} \tag{B7}$$

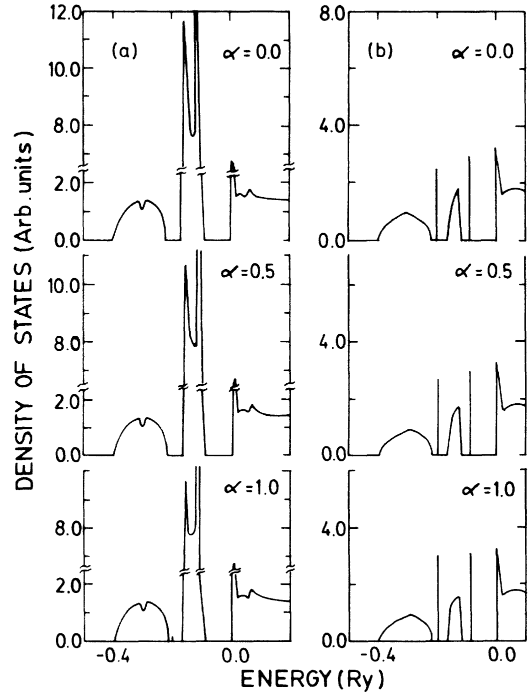

FIG. 6. Local DOS on a single impurity of potential depth (a) 0.3 Ry (type A), and (b) 0.2 Ry, embedded in the KKR-CCPA medium for $x=0.1$, using Eq. (C1). Vertical lines in (b) at -0.2 and -0.1 Ry denote the impurity levels.

In Eqs. (B6) and (B7) $K=\sqrt{E}$ and $\underline{C}\equiv\underline{C}_{\text{eff}}$ and $\underline{b}\equiv\underline{b}^{01}$. Now consider a one-dimensional MT potential,

$$v_n(x)=-V_0^{A(B)}\Theta(r_m-r)\ .$$

The phase shifts are given by

$$\theta_l=-Kr_m+\tan^{-1}\left[\left[\frac{k_l}{K}\right]^{-l}\tan(k_1r_m)\right] \qquad \text{(B8)}$$

where

$$k_1=(E+V_0)^{1/2}\ .$$

The wave functions $\underline{Z}_l(x)$, both inside and outside the MT cell, can also be found analytically and thus the integral

$$\underline{F}_{ll'}=\int_\Omega\underline{Z}_l(x)\underline{Z}_{l'}(x)dx$$

can be evaluated to give

$$\underline{F}_{ll'}=\frac{\delta_{ll'}}{2E\sin^2\Theta_l}\left[\frac{\cos^2(Kr_m+\Theta_l-l\pi/2)}{\cos^2(k_1r_m-l\pi/2)}\left\{r_m+\frac{\sin(2k_1r_m-l\pi)}{2k_1}\right\}+\frac{a}{2}-r_m+(-1)^l\left\{\frac{\sin(Ka+2\Theta_l)-\sin(2Kr_m+2\Theta_l)}{2K}\right\}\right]. \qquad \text{(B9)}$$

The off-diagonal elements of $\underline{F}$ vanish due to opposite parity of the $l=0$ and 1 wave functions.

APPENDIX C: OFF-DIAGONAL TERMS BETWEEN REAL AND EFFECTIVE ATOMS

Let us embed a single atom in the KKR-CCPA medium. We assume the off-diagonal term between real and effective atoms to be of the form

$$\underline{B}^{ij}_{\text{new}}=\underline{B}^{ij}+\alpha(\underline{B}^{ij}_{\text{eff}}-\underline{B}^{ij}),\quad 0\le\alpha\le1\ . \qquad \text{(C1)}$$

The case $\alpha=1$, represents the one which we have adopted in Sec. II C. We have calculated local DOS on this impurity embedded in the KKR-CCPA medium using Eq. (C1) for various impurity potentials with different values of α. In Fig. 6(a), we show the local DOS on A-type impurity (potential depth $=0.3$ Ry) for $x=0.1$ and $\alpha=0.0$, 0.5, and 1.0. We observe that there is some variation in the height of the peaks in the local DOS with α, although there is little qualitative change in the DOS. The variation in the height of the peaks for $\alpha=0.0$ and 1.0 is less than 10%. A similar trend is observed in the case of $x=0.5$. Also, for an impurity of foreign kind, the same conclusion can be drawn from Fig. 6(b), which shows local DOS on the impurity of potential depth 0.2 Ry. Although the basic structure of the local DOS does not change with different choices of the off-diagonal terms between real and effective atoms, we feel that further work is needed to clarify the problem of embedding in the KKR-CCPA medium.

---

*Present address: S. N. Bose National Center for Basic Sciences, DB-17, Sector I Salt Lake, Calcutta 700064, India.

[1] A. Bansil, in *Electronic Band Structure and its Applications,* edited by M. Yussouff (Springer-Verlag, Berlin, 1987), p. 273.

[2] J. S. Faulkner, in *Progress in Materials Science,* edited by J. W. Christian, P. Hassen, and T. Massalski (Pergamon, New York, 1982), Vol. 27, p. 1.

[3] H. Ehrenreich and L. Schwartz, in *Solid State Physics,* edited by H. Ehrenreich, F. Seitz, and D. Turnbull (Academic, New York, 1976), Vol. 31, p. 149.

[4] H. Wright, P. Weightman, P. T. Andrews, W. Folkerts, C. F. J. Flipse, G. A. Sawatzky, D. Norman, and H. Padmore, Phys. Rev. B **35**, 519 (1987).

[5] D. van der Marel, J. A. Jullianus, and G. A. Sawatzky, Phys. Rev. B **32**, 6331 (1985).

[6] J. Banhart, W. Pfeiler, and J. Voitlander, Phys. Rev. B **37**, 6027 (1988).

[7] B. G. Nickel and J. A. Krumhansl, Phys. Rev. B **4**, 4354 (1971).

[8] M. Tsukada, J. Phys. Soc. Jpn. **26**, 684 (1969); **32**, 1475 (1972).

[9] W. H. Butler, Phys. Rev. B **8**, 4499 (1973).

[10] N. F. Berk, J. Shazeer, and R. A. Tahir-Kheli, Phys. Rev. B **8**, 2496 (1973).

[11] A. Gonis and J. W. Garland, Phys. Rev. B **16**, 2424 (1977).

[12] A. Gonis, W. H. Butler, and G. M. Stocks, Phys. Rev. Lett. **50**, 1482 (1983).

[13] A. Gonis, G. M. Stocks, W. H. Butler, and H. Winter, Phys. Rev. B **29**, 555 (1984).

[14] A. Gonis and A. J. Freeman, Phys. Rev. B **29**, 4277 (1984).

[15] B. G. Nickel and W. H. Butler, Phys. Rev. Lett. **30**, 373 (1973).

[16] A. R. Bishop and A. Mookerjee, J. Phys. C **7**, 2165 (1974).

[17] R. Mills and P. Ratanavararaksa, Phys. Rev. B **18**, 5291 (1978).

[18] T. Kaplan, P. L. Leath, L. J. Gray, and H. W. Diehl, Phys. Rev. B **21**, 4230 (1980).

[19] P. L. Leath, in *Excitations in Disordered Systems,* edited by M. F. Thorpe (Plenum, New York, 1981), p. 109; T. Kaplan and L. J. Gray, *ibid.*, p. 129.

[20] A. Mookerjee, in *Electronic Band Structure and its Applications,* edited by M. Yussouff (Springer-Verlag, Berlin, 1987), p. 248.

[21] V. Kumar, A. Mookerjee, and V. K. Srivastava, J. Phys. C **15**,

1939 (1982); P. K. Thakur, A. Mookerjee, and V. A. Singh, J. Phys. F **17**, 1523 (1987).

[22] R. Mills, L. J. Gray, and T. Kaplan, Phys. Rev. B **27**, 3252 (1983).

[23] T. Kaplan and L. J. Gray, Phys. Rev. B **29**, 3684 (1984).

[24] A. Mookerjee, J. Phys. F **17**, 1511 (1987); S. S. Rajput, S. S. A. Razee, R. Prasad, and A. Mookerjee, J. Phys. Condensed Matter **2**, 2653 (1990).

[25] N. Stefanou, R. Zeller, and P. H. Dederichs, Solid State Commun. **62**, 735 (1987).

[26] A. Mookerjee, J. Phys. C **6**, L205 (1973); **6**, 1340 (1973).

[27] L. J. Gray and T. Kaplan, Phys. Rev. B **14**, 3462 (1976); **15**, 6005 (1977); J. Phys. C **9**, L303 (1976); **9**, L483 (1976).

[28] A. Mookerjee, J. Phys. C **9**, 1225 (1976); **19**, 193 (1986); **19**, 275 (1986).

[29] S. S. A. Razee, A. Mookerjee, and R. Prasad (unpublished).

[30] J. S. Faulkner and G. M. Stocks, Phys. Rev. B **21**, 3222 (1980).

[31] A. Gonis and G. M. Stocks, Phys. Rev. B **25**, 659 (1982).

[32] P. K. Thakur and A. Mookerjee, Phys. Rev. B **38**, 3798 (1988).

[33] L. J. Gray and T. Kaplan, Phys. Rev. B **24**, 1872 (1981).

[34] W. H. Butler, Phys. Rev. B **14**, 468 (1976).

[35] In principle, one can embed a cluster of impurities to find charge densities for different configurations of the cluster. The component charge density $\rho^{(\alpha)}(\mathbf{r})$ on a particular impurity α will be different for different configurations of impurities around it. This, in turn, will give us different $v^{(\alpha)}(\mathbf{r})$ for different configurations of the cluster. For example, for a two-atom cluster, $v^{(A)}(\mathbf{r})$ will be different for AA- and AB-type clusters. However, in our formulation, we assume $v^{(A)}(\mathbf{r})$ to be the same for AA- and AB-type clusters. Therefore we do not need different $v^{(\alpha)}(\mathbf{r})$ for different clusters.